Journal of Chromatography A, 658 (1994) 259–270
Elsevier Science B.V., Amsterdam

CHROM. 25 125

Review

Preparative chromatographic separation with moving feed ports

K. Kubota* and S. Hayashi

Department of Chemical Engineering, Faculty of Engineering, Kobe University, Nada-ku 657 Kobe (Japan)

ABSTRACT

The literature on chromatographic separations is reviewed, especially, with regard to experimental and analytically predicted elution curves in a preparative chromatographic separation technique with moving feed ports, although this technique is not very familiar in comparison with the conventional mode. In contrast to the conventional mode, during the feed pulse the feed position is moved continuously up into the column at a velocity that lies between the two solute velocities. A solvent is continuously fed into the bottom of the column. Typical recent studies on liquid and gas chromatographic separation techniques with the moving feed mode for separating binary component systems are discussed and the observed elution curves for these binary systems are compared with those predicted by simulated curves. To predict the observed curves, a set of simple differential equations with and without taking account of mass transfer resistance are presented according to previous workers and the present authors. As a result, the theoretical least chromatographic band spreading was found in the moving feed mode only if mass transfer resistance between the mobile and stationary phases does not participate in the adsorption process. Further, good qualitative agreement was observed between the predicted and the observed curves, showing that the moving feed mode can improve the peak height and the band width of the elution curves compared with the non-moving feed mode (conventional feed mode) with a diluted feed solution, and this improvement depends strongly on the magnitude of the adsorption density and the mass transfer coefficient.

CONTENTS

* Corresponding author.

0021-9673/94/$26.00
SSDI 0021-9673(93)E0438-Z

1. HISTORICAL BACKGROUND

Liquid and gas chromatographic separations for the industrial scale have been developed and used, but these separations have not become an established standard operation for industrial separations. The usual form of elution chromatography is thermodynamically inadequate. As a result, Universal Oil Products developed a simulated counter-current adsorber that is very efficient, and it has been widely used for separating organic components from solutions [1,2]. Although the simulated counter-current system is thermodynamically much more efficient, it is limited to binary separations and is much more complex than elution chromatography.

Recently, much attention has been paid to the processing of multi-component mixtures with this system. Wankat [3] proposed a hybrid system that retains the characteristics of both elution chromatography and the simulated counter-current system stated above. During the feed pulse, the feed position was moved continuously into the bottom of the column. Elution with a solvent was applied when the feed pulse was over. This method reduces irreversible mixing of solutes near the feed point. Wankat [4] extended the method to two-dimensional separations. The proposed method is general and could also be applied to gas chromatography. In actual practice, a segmented column with feed ports at a distance has been used. Wankat and Ortiz [5] studied this scheme in gel permetation chromatography and Ha *et al.* [6] studied it in gas–liquid chromatography.

2. RECENT EXPERIMENTAL APPARATUS FOR PREPARATIVE CHROMATOGRAPHIC SEPARATION WITH MOVING FEED PORTS

Two series of experiments are presented here. One was conducted by Wankat and Ortiz [5] for the separation of cobalt chloride from Blue Dextran 2000 and the other was reported by Ha *et al.* [6] for the separation of the close-boiling compounds diethyl ether and dichloromethane.

Fig. 1 shows a schematic diagram of the chromatographic separation apparatus with moving feed ports. Distilled water was used as the solvent. Experiments were done with total feed times of 60 and 90 s at four different velocities of the feed port and zero feed port velocity (ordinary elution chromatographic separation).

Typical experimental conditions are presented in Table 1 (only those for a 60-s total feed time). Experimental results for a binary component system, *i.e.*, Blue Dextran 2000 and cobalt chloride, are shown in Fig. 2. Sephadex G-25 medium-grade gel was used as the solid stationary phase for all the segmented columns shown in Fig. 1.

From Fig. 2, it can be seen that the moving

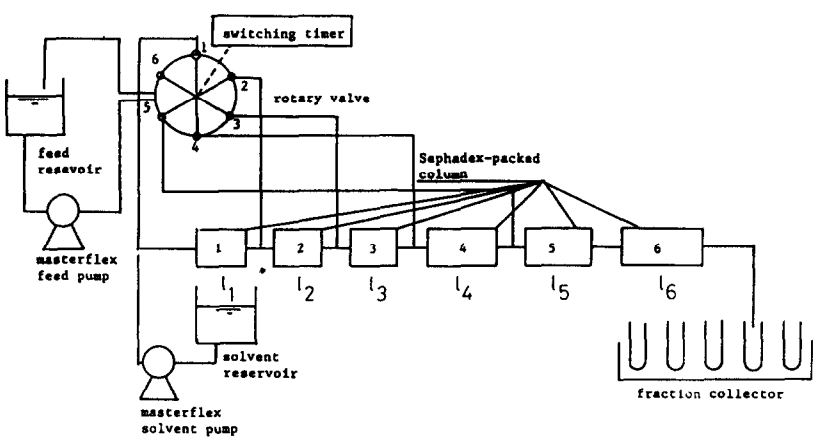

Fig. 1. Moving feed point chromatography apparatus.

TABLE 1

EXPERIMENTAL CONDITIONS FOR SEPARATING BLUE DEXTRAN 2000 AND COBALT CHLORIDE USING SEPHADEX G-25 AS AN ADSORBENT (FROM REF. 5)

Solvent (carrier, water) flow-rate	5.55 cm^3/min		
Feed flow-rate	0.56 cm^3/min		
Feed concentrations (in distilled water):			
Blue Dextran 2000	$5.677 \cdot 10^{-3}$ g/cm^{-3}		
Cobalt chloride	0.1314 g/cm^{-3}		
Total column length, L	18.7 cm		
Column section lengths	$l_1 = l_2 = l_3 = 2.5$ cm; $l_4 = 3.6$ cm; $l_5 = 3.4$ cm; $l_6 = 4.2$ cm		
Injection time to each port:	Port 1	Port 2	Port 3
V_{feed}: 0.125 $cm/s^{-1} = l_1$/injection time	20 s	20 s	20 s
V_{feed}: 0	60 s		

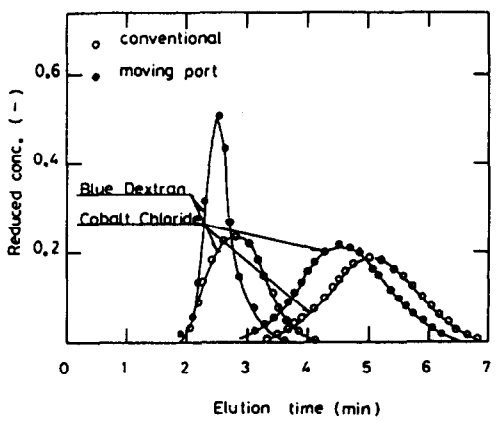

Fig. 2. Traces for gel chromatographic separation with a 60-s total feed time (see Table 1 for details).

feed system has much sharper bands, less dilution of the solutes and better resolution, and cobalt chloride can penetrate more strongly than Blue Dextran 2000 into the adsorbent.

Fig. 3 shows a schematic diagram of the experimental apparatus for separating binary organic components, *i.e.*, diethyl ether (DEE) and dichloromethane (DCM), by gas–liquid chromatography and Table 2 gives the experimental conditions for conventional and moving feed operations.

Fig. 4 shows the experimental results obtained with this scheme. Earlier elution is observed for DEE than DCM, indicating that DCM is more strongly adsorbed than DEE on the adsorbent in both operational modes. The moving mode gives

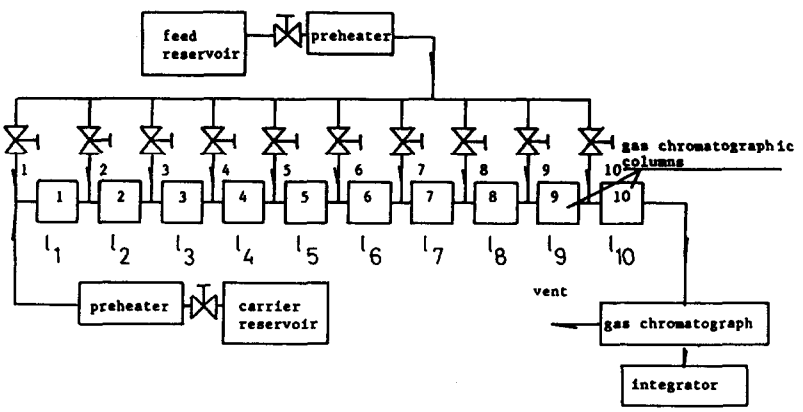

Fig. 3. Schematic diagram of experimental apparatus.

TABLE 2

EXPERIMENTAL CONDITIONS FOR SEPARATING DIETHYL ETHER AND DICHLOROMETHANE USING CHROMOSORB A LOADED WITH 20% DINONYL PHTHALATE AS AN ADSORBENT (FROM REF. 12)

Solvent (carrier, nitrogen) flow-rate	$427.35\ cm/min^{-1}$							
Feed concentrations (in nitrogen):								
DEE	$2.829 \cdot 10^{-4}$ mol/l carrier							
DCM	$1.950 \cdot 10^{-4}$ mol/l carrier							
Total column length, L	260 cm							
Column section lengths	$l_1, \ldots, l_{10} = 26$ cm							
Column diameter	10 mm							
Injection time to each port:	Port 1	Port 2	Port 3	Port 4	Port 5	Port 6	Port 7	
V_{feed}: 13 cm/min = l_1/injection time	2 min	2 min	2 min	2 min	2 min	2 min	2 min	(Fig. 4)
V_{feed}: 0	14 min							
V_{feed}: 13 cm/min = l_1/injection time	Port 1	Port 2	Port 3	Port 4	Port 5	Port 6		
	2 min	2 min	2 min	2 min	2 min	2 min	(Fig. 11)	

much sharper bands, less dilution of the solutes and better resolution.

3. PREDICTION OF ELUTION CURVES OF CHROMATOGRAPHIC SEPARATIONS WITH MOVING FEED PORTS

3.1. Basic equations used for predicting elution curves for the case where there is no mass transfer resistance between the mobile (carrier) and stationary (adsorbent) phases

When mass transfer resistance between the two phases can be ignored, the concentration of an adsorptive component within a column can be described by a familiar equation with appropriate boundary and initial conditions [7]:

$$\varepsilon(\partial C/\partial t) + (1-\varepsilon)\alpha(\partial \bar{C}^*/\partial t) + \bar{\rho}_s(1-\alpha)(1-\varepsilon)x(\partial \bar{q}/\partial t) + \varepsilon\bar{u}(\partial C/\partial z) - \varepsilon(E_D + D_M)(\partial^2 C/\partial z^2) = 0 \quad (1)$$

With the assumption of local equilibrium between solid and fluid, negligible dispersion effects, negligible heat of adsorption and solutes independent of each other, eqn. 1 simplifies to

$$[\varepsilon + (1-\varepsilon)\alpha](\partial C/\partial t) + \bar{\rho}_s(1-\alpha)(1-\varepsilon)(\partial \bar{q}/\partial t) + \varepsilon\bar{u}(\partial C/\partial z) = 0 \quad (2)$$

Instead of eqn. 2, a more simplified local equilibrium model has been proposed by Sherwood *et al.* [8] and can be written as follows, neglecting dispersion effects:

$$(\partial C/\partial t) + [\rho_s(1-\varepsilon)/\varepsilon](\partial q/\partial t) + \bar{u}(\partial C/\partial z) = 0 \quad (3)$$

When local equilibrium exists at all points and all times between the solid phase and the adjacent fluid, an equilibrium relationship $q = f(C)$ can be substituted into eqn. 3 to yield

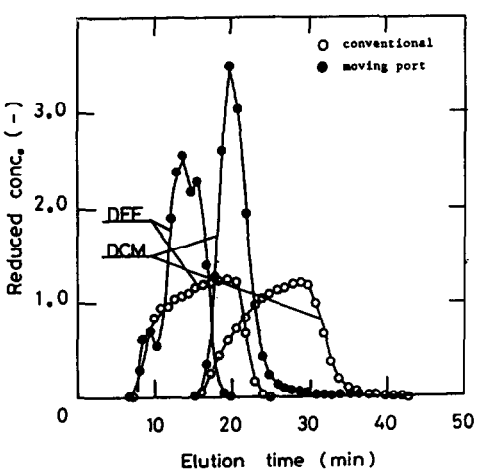

Fig. 4. Comparison of elution profiles for conventional preparative and moving feed injection systems with a total feed time of 14 min (see Table 2 for details).

$$\{1 + [\rho_s(1-\varepsilon)f(C)/\varepsilon]\}(\partial C/\partial t) + \bar{u}(\partial C/\partial z) = 0 \quad (4)$$

Eqn. 5 gives the total derivative with respect to C, and $\partial C/\partial/t$ can be derived from eqns. 4 and 5 and eqn. 6, and a similar equation for $\partial C/\partial z$ can also be derived.

$$(\partial C/\partial t)\mathrm{d}t + (\partial C/\partial z)\mathrm{d}z = \mathrm{d}C \quad (5)$$

$$\partial C/\partial t = \frac{\begin{vmatrix} 0 & \bar{u} \\ \mathrm{d}C & \mathrm{d}z \end{vmatrix}}{\begin{vmatrix} 1 + [\rho_s(1-\varepsilon)f'(C)/\varepsilon] & \bar{u} \\ \mathrm{d}t & \mathrm{d}z \end{vmatrix}} \quad (6)$$

There are certain characteristic directions in the zt plane that make the denominator equal to zero, and in this event the numerator must also be zero if $\partial C/\partial t$ is to be finite. Then $\mathrm{d}C$ will be zero. Hence C is constant along the characteristics corresponding to

$$\mathrm{d}z/\mathrm{d}t = \bar{u}/\{1 + [\rho_s(1-\varepsilon)f'(C)/\varepsilon]\} \quad (7)$$

When equilibrium relationships are restricted to a linear type although eqn. 7 can hold for general functions of equilibrium relationships, this equation can be described by

$$\mathrm{d}z/\mathrm{d}t = \bar{u}\{1 + [(1-\varepsilon)m/\varepsilon]\} = (\bar{u}_s + \bar{u}_f)/\{1 + [(1-\varepsilon)m/\varepsilon]\} \quad (8)$$

Here a linear-type adsorption isotherm, $q\rho_s = m\mathrm{C}$, is assumed, where m is the distribution coefficient and the left-hand side represents the concentration wave velocity. When there is an efficient mass transfer rate between the two phases, fluid marked by a certain composition travels through the column without a change in wave velocity.

3.2. Basic equations used for predicting elution curves for the case where there is mass transfer resistance between both phases

Incorporating a mass transfer resistance into eqn. 3, a simple set of equations (eqns. 9 and 10) to be solved simultaneously to predict an elution curve for a component of interest can be derived:

$$\partial C/\partial t + (u/\varepsilon) + (K_f a_v/\varepsilon)(C - C^*) = 0 \quad (9)$$

$$\partial C^*/\partial t = K_{fav}(C - C^*)/m(1-\varepsilon) \quad (10)$$

where $K_f a_v$ is the overall volumetric mass transfer coefficient. When the mass transfer rate is infinite, C^* can be regarded as C, eqns. 9 and 10 lead to eqn. 3 and an elution curve can be produced with arbitrarily given numerical values for m, ε, $K_f a_v$ and column length L.

Based on the equations in Sections 3.1 and 3.2, simulated elution curves can be discussed as follows. Here a column of length 0.7 m is segmented and arranged as shown in Fig. 5 (case 1). The feed pulse is subdivided into five equal parts and input at $z = 0$, 0.075, 0.15, 0.225 and 0.3 m for 210 s each, keeping the carrier and feed solution superficial velocities and feed concentration at 0.00024 m/s, 0.00016 m/s and 0.71428 kmol/m^3, respectively. During the course of the first injection the fluid rate equals the sum of 0.00024 and 0.00016 m/s; however, when the injection is switched to the second column, only the carrier flow-rate, 0.00024 m/s, remains in the first column, and when the injection is switched to the third column, the carrier flow-rate remains in the first and second columns while the remainder of all column's flow-rates are the sum of 0.00024 and 0.00016 m/s. Analogous variations in the liquid flow-rates continue until the injection port is switched to the segmented final column, from which elution will be developed. Three characteristic lines according to eqn. 8 are also shown in Fig. 6, where two ordinary injection modes (non-moving mode) and the moving mode are compared. As for the moving mode, a change in the fluid velocities is considered whenever an injection port is moved as shown in the figure, showing that five pairs of characteristic lines are almost overlapped and suggesting that elution will start at 1900 s and end at 2280 s after the beginning of the first injection. Therefore, the elution time interval is 380 s as shown (characteristic 1). Here the value for m is arbitrarily set at 0.53. Characteristics 2 and 3 show two differ-

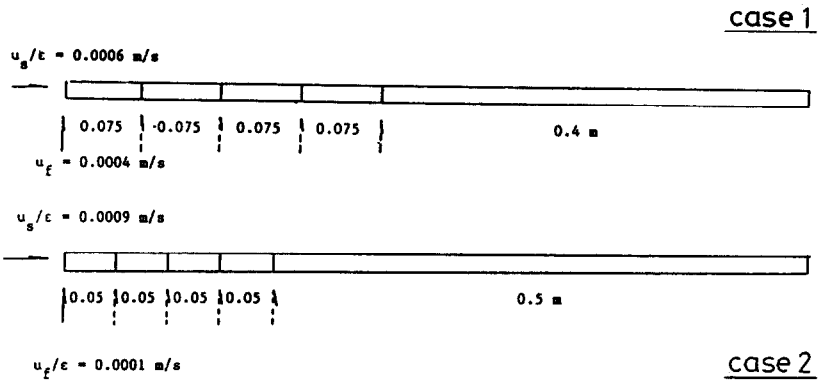

Fig. 5. Column alignments for the simulation of the moving feed mode [case 1, (0.075 m × 4) + 0.4 m; case 2, (0.05 m × 4) + 0.5 m].

ent cases of non-moving feed modes with the total injection mass kept at 0.12 kmol/m^2 of column.

The loading conditions for characteristic 2 are as follows: after a pulse of 420 s with a feed concentration $C_f = 0.71428$ kmol/m^3 and a superficial velocity of 0.0004 m/s has been carried out, the carrier with a superficial velocity of 0.00024 m/s is introduced into the first column. Elution will start at *ca.* 1830 s, and the elution time interval cut by characteristic lines is 650 s as shown. The loading conditions for characteristic 3 are as follows: after a pulse of 700 s with feed concentration $C_f = 0.71428$ kmol/m^3 and a superficial velocity of 0.00024 m/s has been carried out, the carrier with the same velocity is continuously introduced into the first column. Elution will start and end at 2100 and 2800 s, respectively, as shown. It can be seen that the narrowest elution time interval is observed in the moving feed mode, indicating that a curve with a higher peak and a narrower band width is eluted compared with the other mode. Other characteristic lines are shown in Fig. 7 where instead of 0.53 for m, 0.79 is used to produce the characteristic lines with all other numerical values kept the same as in Fig. 6. Similar statements made for Fig. 6 hold for Fig. 7, showing that a slightly broadened band is predicted because the characteristic lines are not as overlapped as those in Fig. 6. On the basis of the local equilibrium model, a more detailed discussion on the per-

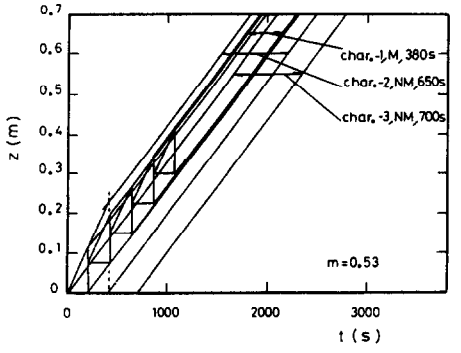

Fig. 6. Characteristic lines for $m = 0.53$. Total injection mass = 0.12 kmol/m^2 of column; injection time on each port = 210 s.

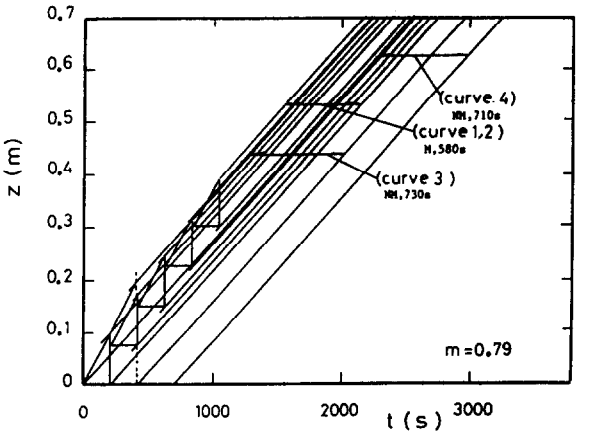

Fig. 7. Characteristic lines for $m = 0.79$. Total injection mass = 0.12 kmol/m^2 of column; injection time on each port = 210 s.

formance of the moving feed mode can be obtained for Fig. 7 in a previous paper [9].

When mass transfer resistance is considered, the equations to be solved are eqns. 9 and 10. Fig. 8 shows the breakthrough curves produced for varying overall capacity mass transfer coefficient $K_f a_v$ and distribution coefficient m, with the feed concentration, superficial fluid velocity and column length kept constant at 0.5 kmol/m^3, 0.0004 m/s and 0.5 m, respectively.

According to Sherwood *et al.* [8], the analytical breakthrough curves in terms of reduced concentration can be represented as

$$C/C_0 = J(\alpha,\beta) = 1 - \exp(-\beta)\int_0^{\alpha} \exp(-\xi) I_0(2\sqrt{\beta\xi})\, d\xi \quad (11)$$

where $\alpha = K_f a_v L/u$ and $\beta = [K_f a_v/m(1-\varepsilon)][t - (L/\bar{u})]$. The curves produced according to the above equation are shown in Fig. 8. The calculation curves according to plate theory are as follows. As shown by Said [10,11], when an adsorption column is equivalent to a plate column consisting of N theoretical plates and the mass of the liquid which has crossed any plate any time is dw, then the differential material balance around the first plate is

$$C_0\, dw - C_1\, dw = (S\, dq_1/N) + (V\, dC_1/N) \quad (12)$$

where C_0 and the C_1 denote the concentrations of the liquid entering and leaving the first plate, respectively, and in terms of the present notation this equation can be rewritten as

$$\bar{u}\, dt/\{[(1-\varepsilon)Lm/\varepsilon N] + (L/N)\} = dC_1/(C_0 - C_1) \quad (13)$$

When at the beginning of the adsorption process the concentration on the 1st, 2nd, 3rd, . . . , Nth plates are $\bar{C}_1$, $\bar{C}_2$, $\bar{C}_3$, . . . , $\bar{C}_N$, the above equation can be solved to give C_1 as follows:

$$C_1 = C_0 - (C_0 - \bar{C}_1)\exp(-At) \quad (14)$$

where

$$A = \bar{u}/\{[(1-\varepsilon)Lm/\varepsilon N] + (L/N)\}$$

Continuing up to the Nth plate, we obtained the concentration

$$C_N = C_0 - \{[(At)^{N-1}(C_0 - \bar{C}_1)/(N-1)!] + [(At)^{N-2}(C_0 - \bar{C}_2)/(N-2)!] + [(At)^{N-3}(C_0 - \bar{C}_3)/(N-3)!] + , \ldots , + [(At)^{N-N}(C_0 - \bar{C}_N)/(N-N)!)]\}\exp(-At) \quad (15)$$

should be noted that Said [10,11] does not

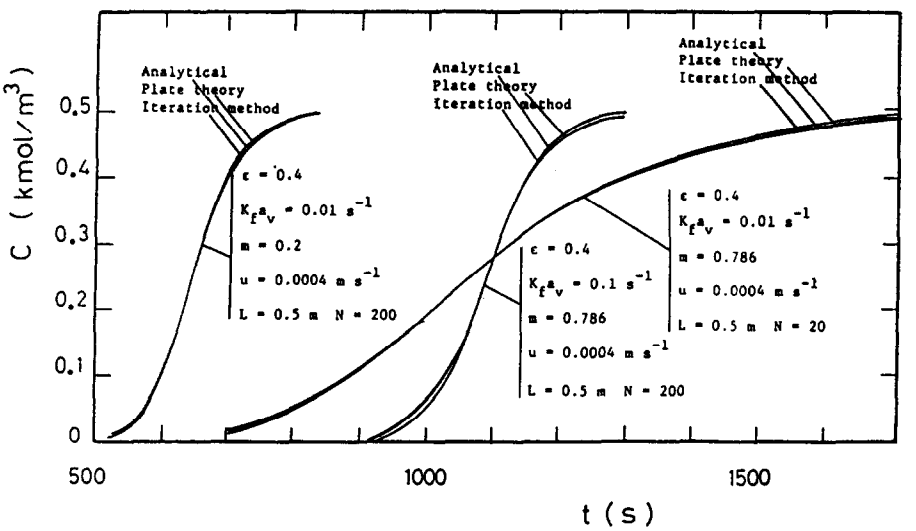

Fig. 8. Breakthrough curves based on three calculation methods.

consider the voidage effect in the derivation of eqns. 12–15. The breakthrough curves for several assigned values of N were generated by using eqn. 15. It can be deduced that the breakthrough curves for $K_f a_v = 0.01\ s^{-1}$ and $0.1\ s^{-1}$ (column length $L = 0.5$ m and $m = 0.79$) almost coincide with those for $N = 20$ and 200, respectively, and the curve for $K_f a_v = 0.01\ s^{-1}$ and $m = 0.2$ coincides with that for $N = 200$. More generally, a theoretical plate number N can be determined from an elution curve with appropriate values for $K_f a_v$ and m by the equation

$$N = 16\,(t_R/w)^2. \tag{16}$$

as had been done in previous work [12,13], where t_R is the distance from injection to peak maximum and w is the length at the baseline cut by the two tangents of a peak.

The breakthrough curves based on the plate theory are shown in Fig. 8. Good agreement is observed in comparison with other curves according to other methods. The curves produced according to iteration method which resembles the "stop and go" method employed in previous work [14] are also shown in Fig. 8. This method is as follows [15]. A column is subdivided into N stages, and each stage is ΔL long. Δt is the time interval required by a fluid element to travel ΔL. The mass entering the first stage during Δt is given by $\bar{u}\varepsilon A C_0\,\Delta t$, while the mass that is transfered to the solid phase during Δt is given by $K_f a_v A\,\Delta L(C_0 - C_0^*)\,\Delta t$. From the material balance on the solid phase, eqn. 17 can be derived. Substituting the linear relationship $q\rho_s = mC$ into this equation gives eqn. 18, and solving for C_1^*, gives eqn. 19.

$$(1-\varepsilon)A\,\Delta L\rho_s(q_1 - q_0) = K_f a_v A\,\Delta L(C_0 - C_0^*)\,\Delta t \tag{17}$$

$$m(1-\varepsilon)A\,\Delta L(C_1^* - C_0^*) = K_f a_v A\,\Delta L(C_0 - C_0^*)\,\Delta t \tag{18}$$

$$C_1^* = [K_f a_v (C_0 - C_0^*)\,\Delta L/m(1-\varepsilon)\bar{u}] + C_0^* \tag{19}$$

On the other hand, eqn. 20 can be derived from the material balance on the liquid phase around the first stage, and solving the equation for C_1 gives eqn. 21.

$$\bar{u}\varepsilon A C_0\,\Delta t - K_f a_v A\,\Delta L(C_0 - C_0^*)\,\Delta t = \bar{u}\varepsilon A C_1\,\Delta t \tag{20}$$

$$C_1 = [\bar{u}\varepsilon C_0 - K_f a_v\,\Delta L(\bar{C}_0 - C_0^*)]/\bar{u}\varepsilon \tag{21}$$

A simple cyclic loop is coupled to this method to enhance the accuracy of the calculation and to save computation time. The concentration of the liquid entering the first stage, C_0, is used as the starting value for the $\bar{C}_0$ in the parentheses in eqn. 21, and the concentration of the liquid leaving from the stage, C_1, is estimated from the same equation. The arithmetic mean $\bar{C}_0 = (C_1 + C_0)/2$ is calculated, which in turn is substituted into $\bar{C}_0$ in the same equation to obtain C_1 for the second cycle. Five cycles were found to be enough to obtain the converged value for C_1 with a permissible error. The converged $\bar{C}_0$ was substituted into C_0 in eqn. 19 to calculate the concentration C_1^*. C_1 was used as the concentration of the fluid entering the second stage where the same cyclic calculation was carried out. The remainder of the stages up to the Nth were calculated in the same fashion. The calculated curves based on the mass balance method, designated the iteration method, are shown in Fig. 8, where fair agreement is observed among three curves, from which both the iteration and plate theory methods can be used to predict elution curves.

Taking the numerical values for $K_f a_v$ and m and column alignment for case 1 in Fig. 5 into account, the plate number for each segment can be alloted as $N_1 = 30$, $N_2 = 30$, $N_3 = 30$, $N_4 = 30$ and $N_5 = 160$.

When the injection port has moved to the second port after the first injection, the superficial velocities for the up- and downstream sides at this port become different. The same situation arises whenever the injection port is successively switched upstream. According to eqn. 15, the calculation is straightforward because in this instance the variation in the fluid velocity can be handled implicitly by this equation, in which the theoretical plate number is never affected by the fluid velocity.

Curve 1 in Fig. 9 shows the elution curve for which the characteristic lines are shown as curves 1, 2 in Fig. 7, and curve 2 shows the elution

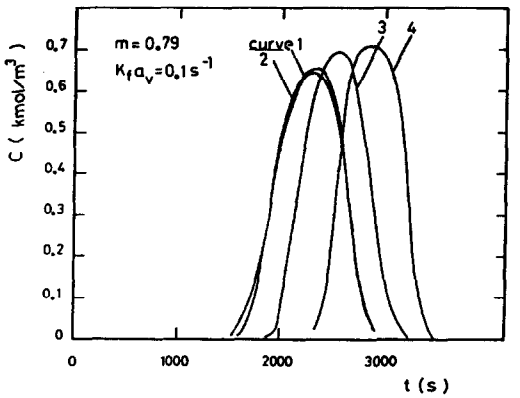

Fig. 9. Elution curves. Curve 1: moving feed mode ($N_1 = 30$, $N_2 = 30$, $N_3 = 30$, $N_4 = 30$, $N_5 = 160$). Curve 2: moving feed mode ($N_1 = 60$, $N_2 = 60$, $N_3 = 60$, $N_4 = 60$, $N_5 = 320$). Curves 3 and 4: non-moving feed mode.

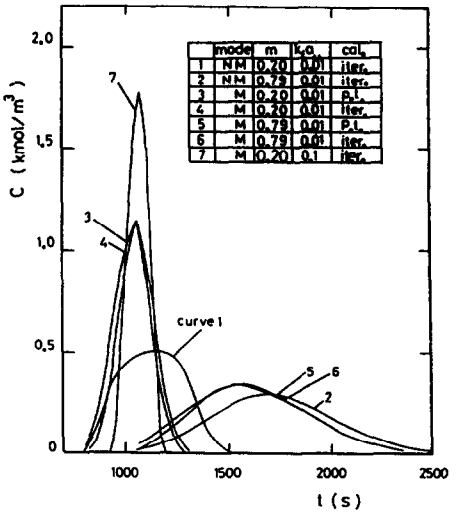

Fig. 10. Effect of mass transfer capacity coefficient $K_f a_v$ and slope of linear adsorption isotherm m on elution curve (case 2 in Fig. 5, injection time on each port = 87.5 s, total injection time = 437.5 s, total injection mass = 0.0875 kmol/m^2 of column).

curve when plate number for each segment is doubled, resulting in only a very slight improvement in peak height. Curves 3 and 4 show the result for the non-moving feed modes for which the characteristic lines are also shown in Fig. 7. From curves 1–4 in Fig. 9, one can suggest that the performance of the moving feed mode can approach that of the non-moving feed mode, but the former cannot overcome the latter as long as only a slight effect of the mass transfer resistance in terms of $K_f a_v$ participates in the adsorption process. This conclusion supports the predictions reported by Geldart *et al.* [9].

Fig. 10 shows the effect of the value of m on the elution curve. Here the superficial velocities of the carrier and the feed solution with a concentration of 5.0 kmol/m^3 are selected as 0.00036 and 0.00004 m/s. The alignment of the five columns consisting of four short columns of 0.05 m and one long column of 0.5 m (case 2 in Fig. 5) was considered for simulation. Each injection pulse interval is kept at 87.5 s (injection time = 437.5 s, total injection mass = 0.0875 kmol/m^2 of column). Curves 1 and 2 show the results for the non-moving feed mode where, after a total injection time of 437.5 s with a superficial velocity of 0.0004 m/s (concentration of feed solution kept at 0.5 kmol/m^3) has elapsed, the carrier with the same velocity stated above is continuously fed into the first column. The elution curve with the larger m shows greater spreading, which does not contradict the ordinary concepts of liquid chromatography. Curves 3 and 4 are the results based on the moving feed mode, which show significant improvements in peak height and band width compared with curve 1. The two curves obtained by the two different methods seem almost to coincide, indicating that the calculation methods presented here would be reliable for predicting chromatographic elution curves. Curves 5 and 6 show the results of the moving feed mode for $m = 0.79$ and $K_f a_v = 0.01$ s^{-1}. When curves 5 and 6 are compared with curve 2, in contrast to the former case (curves 1, 3 and 4), no remarkable improvements in peak height and band width are observed, but a shifting of the elution time interval is noticed.

3.3. Comparison of the experimental elution curves with the analytical elution curves

From Table 1, it can be seen that a fraction of the superficial velocity of the feed solution, containing the two components, to that of the carrier equals 0.1, which agrees with the loading conditions for Fig. 10 although the segmented column arrangement in Fig. 1 (Table 1) does not

match that used for the simulation in Fig. 10. The experimental curves for cobalt chloride resemble curves 5, 6 and 2 in Fig. 10, whereas the experimental curves for Blue Dextran 2000 resemble curves 3, 4 and 1 in Fig. 10, indicating that cobalt chloride would be more strongly adsorbed on the adsorbent than Blue Dextran 2000; in other words, cobalt chloride would show a larger m than Blue Dextran 2000 on this adsorbent. Unfortunately, in the original paper containing Table 1 [5] the authors do not discuss their results in terms of m and $K_f a_v$, hence a quantitative comparison between the simulation and experimental curves is not feasible. From Table 2, it can be also seen that the ratio of the superficial velocity of the feed solution to that of the carrier equals 0.09, which again almost agrees with the loading conditions for Fig. 10, although the segmented column arrangement used in Fig. 2 (Table 2) does not match that in Fig. 10. Qualitatively, the peak height and the band width in the conventional mode can be significantly improved by the moving mode, and it can be experimentally observed for both components, DEE and DCM. The curves for DEE and DCM resemble curves 3, 4 and 1, simulated in Fig. 10.

Fig. 11 shows a comparison between the observed and simulated curves of the moving mode [6]. The loading conditions are also given in Table 2. The calculation method is the plate theory method, where number of plates required for predicting the elution curve is determined

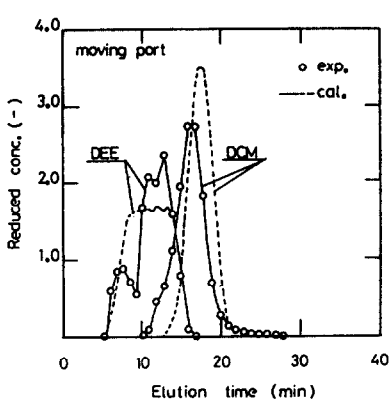

Fig. 11. Comparison of experimental and calculated elution profiles for moving injection system [see Table 2 (bottom) for details].

with eqn. 16. In spite of some deviations between the simulated and observed profiles, the theoretical results are in relatively good agreement with the data. However, in the original report [6], it was not clearly stated how the authors mathematically handled a change in the superficial velocities for the up- and downstream sides at an injection port.

4. CONCLUSIONS

It can be concluded from Figs. 1, 2 and 10 that the moving feed mode can significantly improve the elution curve compared with the conventional feed mode; however, this statement holds for a feed solution diluted with carrier, as can be seen in tables 1 and 2. When the chromatographic performance of the moving feed mode is compared with that of the conventional mode, with the total injection loading mass kept constant, the former would be superior to the latter only if the mass transfer resistance does not participate in the adsorption process as simulated and predicted in Figs. 6 and 8. However, the performance of the moving feed mode cannot exceed that of the non-moving feed mode as long as the resistance participates in the adsorption process, as simulated in Fig. 9, which is supported by ref. 9.

The distribution coefficient m is the ratio of the mass of a component within unit volume of an adsorbent to the mass within unit volume of a fluid phase. If a chromatographic separation system in which the numerical values of m and $K_f a_v$ are much larger than those handled in the present simulation is available, the narrowest band width of the moving feed mode, predicted in Figs. 6 and 7, could be experimentally supported and verified, as the overloading that would occur when the five sets of characteristic lines are confined into the narrowest band width may be avoidable.

5. SYMBOLS

A	cross-sectional area of empty column (m^2)
a_v	area for mass transfer per unit empty column volume (m^2/m^3)

C	concentration of liquid (kmol/m^3)
C_f	concentration of feed solution (kmol/m^3)
C_0	concentration of liquid entering 1st stage (kmol/m^3)
C_1	concentration of liquid leaving 1st stage or 1st plate (kmol/m^3)
C^*	concentration of liquid at liquid–solid interface in equilibrium with solid phase (kmol/m^3)
C_0^*	concentration of liquid at liquid–solid interface in equilibrium with initial solid-phase concentration (kmol/m^3)
C_1^*	concentration of liquid at liquid–solid interface in equilibrium with solid-phase concentration at completion of adsorption on 1st stage (kmol/m^3)
$\bar{C}_1, \bar{C}_2, \bar{C}_3, \ldots, \bar{C}_N$	concentration of liquid (=concentration of liquid at liquid–solid interface in equilibrium with solid-phase concentration) at the beginning of adsorption on 1st, 2nd, 3rd, . . . , Nth plates (kmol/m^3)
$\bar{C}^*$	concentration of liquid at liquid–solid interface in equilibrium with solid-phase concentration ($=\bar{q}\bar{\rho}_s$) (kmol/m^3)
E_D	eddy diffusivity (m^2/s)
E_M	mass molecular diffusivity (m^2/s)
$f(C)=f(q\rho_s)$	general isotherm function
$f'(C)=f'(q\rho_s)$ $=\mathrm{d}(q\rho_s)/\mathrm{d}C$	1st derivative of general isotherm function
$K_f a_v$	overall capacity mass transfer coefficient (1/s)
l	individual segmented column length (m)
$m=q\rho_s/C$	slope of linear isotherm
N	stage or plate number
N_1–N_5	plate number required for segmented columns 1–5
q	adsorption density (kmol/kg wet adsorbent)
q_0	adsorption density in equilibrium with C_0^* (kmol/kg wet adsorbent)
q_1	adsorption density in equilibrium with C_1^* (kmol/kg wet adsorbent)
$\bar{q}$	adsorption density (kmol/kg dry adsorbent)
S	total mass of adsorbent (kg wet solid per column)
t	real time (s)
t_R	elapsed time from injection to that giving peak maximum (s)
u	superficial velocity of liquid (m/s)
u_f	superficial velocity of feed solution (m/s)
u_s	superficial velocity of solvent or carrier (m/s)
$\bar{u}=u/\varepsilon$	average interstitial velocity of liquid (m/s)
$\bar{u}_f=u_f/\varepsilon$	average interstitial velocity of feed solution (m/s)
$\bar{u}_s=u_s/\varepsilon$	average interstitial velocity of solvent or carrier (m/s)
V	total void volume (m^3/column)
V	l/injection time (m/s)
w	time interval cut by two tangents of peak (s)
z	distance from entrance (m)
α	intraparticle void fraction
α	dimensonless parameter in eqn. 11
β	dimensionless parameter in eqn. 11
ΔL	length of each stage (m)
Δt	time interval required by a liquid element to travel ΔL (s)
ε	interparticle void fraction
M	pertaining to moving feed mode
N	pertaining to non-feed mode
ξ	independent variable in integration in eqn. 11

REFERENCES

1 D.B. Broughton, R.W. Neuzil, J.M. Pharis and C.S. Breasley, *Chem. Eng. Progr.*, 66, No. 9 (1970) 70.

2 A.J. DeRosset, R.W. Neuzil and D.J. Korous, *Ind. Eng. Chem., Process Des. Dev.*, 15 (1976) 261.

3 P.C. Wankat, *Ind. Eng. Chem., Fundam.*, 16 (1977) 468.
4 P.C. Wankat, *Sep. Sci.*, 12 (1977) 553.
5 P.C. Wankat and P.M. Ortiz, *Ind. Eng. Chem., Progress Des. Dev.*, 21 (1982) 416.
6 H.Y. Ha, K.H. Row and W.K. Lee, *Sep. Sci.*, 22 (1987) 1281.
7 B. Baker and R.L. Pigford, *Ind. Eng. Chem., Fundam.*, 10 (1971) 283.
8 T.K. Sherwood, R.L. Pigford and C.R. Wilke, *Mass Transfer*, McGraw-Hill, Kogakusha, Tokyo, 1975, Ch. 10.
9 R.W. Geldart, N.-H. L. Wang and P.C. Wankat, *Chem. Eng. Commun.*, 58 (1987) 273.
10 A.S. Said, *AIChE J.*, 2 (1956) 477.
11 A.S. Said, *AIChE J.*, 5 (1959) 69.
12 H.Y. Ha, K.H. Row and W.K. Lee, *Sep. Sci.*, 22 (1987) 141.
13 L.R. Snyder and J.J. Kirkland, *Introduction to Modern Liquid Chromatography*, Wiley, New York, 1974, Ch. 2.
14 G.H. Miller and P.C. Wankat, *Chem. Eng. Commun.*, 31 (1984) 21.
15 K. Kubota and S. Hayashi, *Can. J. Chem. Eng.*, 68 (1990) 420.